

Anisotropies of Nonpolar a-Plane GaN LEDs in Electrical and Optical Properties

Soohwan Jang^{a*}, Kwang Hyeon Baik^b, Sung-Min Hwang^b, S. J. Pearton^c, and F. Ren^d

^aDepartment of Chemical Engineering, Dankook University, Yongin, 448-701, Korea

^bOptoelectronics Labs, Korea Electronics Technology Institute, Sunghnam, Gyeonggi 463-816, Republic of Korea

^cDepartment of Materials Science and Engineering, University of Florida, Gainesville, FL 32611

^dDepartment of Chemical Engineering, University of Florida, Gainesville, FL 32611

*jangmountain@dankook.ac.kr, tel: 82-31-8005-3623

Keywords: Nonpolar, a-plane GaN, LEDs, BPSF, anisotropy

Abstract

Electrical and optical properties of a-plane GaN on r-plane (1102) sapphire substrates according to m- and c-axes are reported. Ohmic contact resistances were measured using TLM (transfer line method) contacts oriented toward both m - and c-directions of a-plane GaN. The lowest specific contact resistances of $\sim 10^{-5} \Omega\text{cm}^2$ were obtained when annealed at 700 °C, and the specific contact resistances increased with temperature after 700 °C. It is found that the sheet resistance along c-axis of a-plane GaN is much higher than the m-axis of a-plane GaN. This is due to the carrier scatterings by BPSFs (basal plane stacking faults) in the direction perpendicular to the c-axis. A-plane GaN based LEDs aligned to m- and c-axes were fabricated and the output powers of devices for each direction were compared. The presence of BPSFs significantly influences electrical and optical performances of the devices.

INTRODUCTION

There are great current interests in nonpolar GaN due to its promise for eliminating internal electric fields, which are present in conventional c-plane III-nitrides [1]. In the polar crystal orientations, both spontaneous and piezoelectric polarization electric fields induce the quantum-confined Stark effect (QCSE), resulting in the reduction in radiative recombination rates in quantum wells (QWs) used as active layers in LEDs [2]. Nonpolar GaN has applications for light-emitting diodes (LEDs), where there is improved wavelength stability with high injection current in non-polar devices and in AlGaIn/GaN transistors, where better control of electron channel is available [2]. Also, a-plane GaN is an attractive material for hydrogen sensing since nitrogen atoms which have higher affinity to hydrogen than gallium exist on the surface [3]. The growth of nonpolar GaN films is quite challenging due to in-plane strain anisotropy, which leads to a high density of extended defects and rough surface morphology. Threading dislocations of nonpolar nitride films are more pronounced than those of c-plane (0001) GaN

films. Furthermore, heteroepitaxial nonpolar GaN films on SiC, sapphire, and LiAlO substrates suffer from stacking faults, which include prismatic stacking faults (PSFs) and basal plane stacking faults (BPSFs) [4-7]. In the nucleation step, they are formed at the interface between GaN and substrate and propagate into the GaN surface. Spatially, intrinsic I₁ type BPSFs are most often observed in the direction perpendicular to the c-axis [0001] in faulted nonpolar GaN films [8-9]. It is obvious that the electrical and optical properties of nonpolar GaN films are strongly influenced by the presence of BSFs, which results in anisotropies of conductivity and optical emission in the directions parallel and perpendicular to the c-axis of a-plane GaN. Also, it is very important to understand how BSFs electrically and optically affect nonpolar nitride films for practical applications of optoelectronic devices.

In this work, we report on the effects of BPSFs on the electrical anisotropy of faulted a-plane GaN films on r-plane sapphire substrates and the device characteristics of nonpolar a-plane GaN LEDs. We find that the sheet resistance along the c-axis is two times higher than that along the m-axis for a-GaN wafer and the device with linear p- and n- contacts parallel to c-axis shows higher current and luminous output intensity.

EXPERIMENTS

For Ohmic contact study, 4.5 μm thick Si-doped a-GaN epitaxial layers were grown on r-plane (1102) sapphire substrates utilizing a two-step growth method by MOCVD. Trimethylgallium, ammonia, and trimethylindium were used as Ga, N, and In sources, respectively. A high-temperature buffer layer was deposited at 1050°C with high V/III ratio to promote island-like growth. Subsequent second buffer layer was grown with higher lateral growth rate to improve the crystal quality and surface flatness. The electron concentration and the mobility obtained from Hall measurements with van der Pauw method were $\sim 3 \times 10^{18} \text{ cm}^{-3}$ and 127 $\text{cm}^2/\text{V}\cdot\text{s}$. Ohmic contacts consisted of Ti (200Å)/Al (400Å)/Ni (200Å)/Au (800Å) deposited by e-

beam evaporation and patterned by lift-off to form TLM patterns with $100 \times 100 \mu\text{m}$ pads separated by spacings from 2-16 μm . Mesas were formed by Cl_2/Ar inductively coupled plasma etching to provide electrical isolation of the contact pads. The TLM patterns were patterned with various azimuthal angles as shown in the inset of Figure 2. These contacts were subsequently annealed at temperatures from 400-800°C for 60 secs under flowing N_2 in a Solaris 150 Rapid Thermal Processing system from Surface Science Integration. Nonpolar a-plane InGaN-GaN LEDs on r-plane sapphire substrates were grown by MOCVD, and experimental details with QW structures had been previously reported [10].

RESULTS AND DISCUSSIONS

The slate-like surface morphology of a-plane GaN aligned parallel to the c-axis is observed, which is typical in nonpolar GaN films. The TLM patterns were oriented along either the c- or m-axis directions. The contacts were rectifying prior to annealing at 600°C and became Ohmic with a minimum resistance around 700°C. The specific contact resistance decreased up to $\sim 650\text{-}700^\circ\text{C}$ in both cases, with a lowest specific contact resistance of $\sim 10^{-5} \Omega\text{-cm}^2$. The minimum in the specific contact resistance with annealing temperature is most likely related to the formation of low resistance phases of TiN at the interface with the GaN. Annealing at higher temperatures leads to higher contact resistance, which corresponds to extensive intermixing of the contact metallurgy.

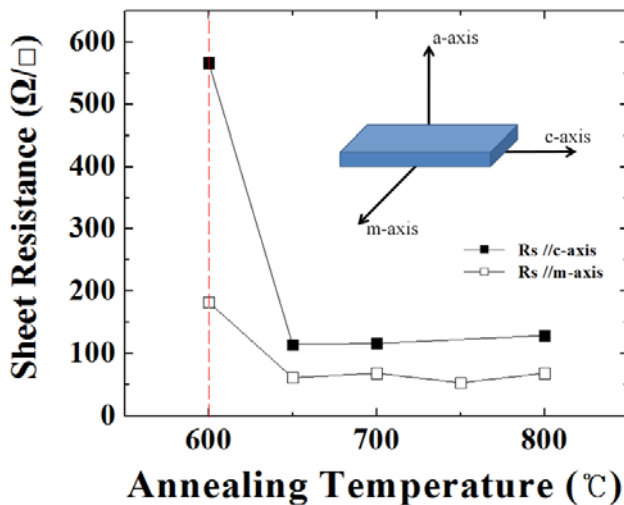


Figure 1. Sheet resistance of a-plane GaN according to annealing temperature for the TLM patterns parallel to both c- and m-axes.

Figure 1 shows the sheet resistance data for the c and m-axis orientations of a-GaN, which shows significant electrical anisotropy in the two directions. It is found that the

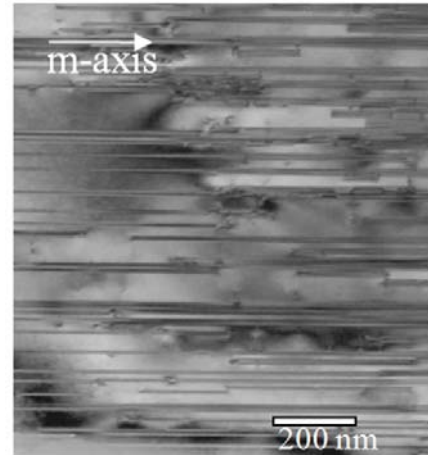


Figure 2. Plan-view TEM image of a-plane GaN

sheet resistance along the c-axis is two times higher than the one along the m-axis when anneal at 700°C, possibly due to the carrier scattering by BPSFs in the direction perpendicular to the c-axis. McLaurin *et al.* suggested that the anisotropic conductivity of faulted nonpolar GaN films might result from BPSFs whose band structures are similar to zincblende GaN. The interface between BPSF and matrix wurtzite GaN induces the band edge discontinuity, and thus hampers carrier transport to the c-axis direction [11-12]. The plan-view image of transmission electron microscopy in figure 2 presents that BPSF of our a-GaN films exists along m-axis and has a density of $1.4\text{-}3.2 \times 10^5 \text{ cm}^{-1}$.

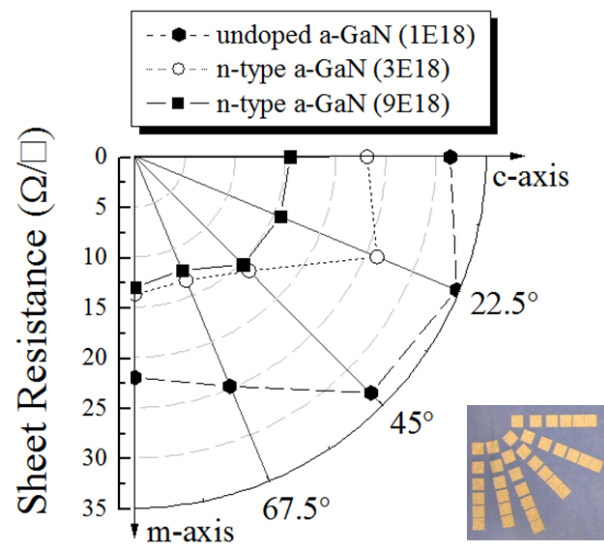


Figure 3. Sheet resistances of a-plane GaN according to azimuthal angles.

Figure 3 indicates the sheet resistance data for various azimuthal angles between the c-axis and the m-axis directions for different doping samples. These results confirm that there exists significant electrical anisotropy with azimuthal angle between the c and m-axis directions for a-GaN, even in the case of highly n-doped films. It is

interesting that the resistance peaks at 22.5deg. It could be related to interfacial roughness at the BPSF interface, which might enhance the scattering of electrons moving along specific directions.

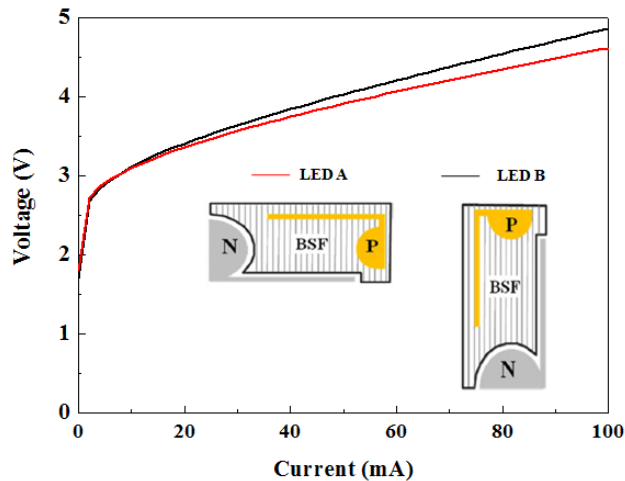


Figure 4. I-V curves of LEDs parallel to c- and m-axes

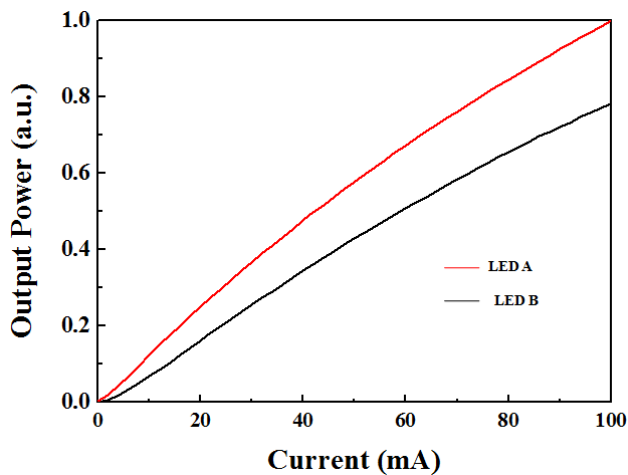


Figure 5. L-I curves of LEDs parallel to c- and m-axes

Figure 4 and 5 show current-voltage (I-V) and light output-current (L-I) characteristics of a-plane GaN LEDs aligned parallel to the c-axis (LED A) and the m-axis (LED B), which are illustrated in figure 4 (insets). On-wafer measurements have shown that the output power of LED A is 50% higher than that of LED B at 100 mA, respectively. It mainly results from nonuniform electron injections due to carrier scatterings by BPSFs in a-plane GaN. The I-V curve in figure 4 shows that the series resistance of LED A (15.4 Ω) is lower than that of LED B (17.9 Ω). Figure 6 confirms that the spatial light distributions for both LEDs are different. The top-view images of the spatial light distributions of LED A and LED B were collected and analyzed using a high-resolution camera (ML4317) and beam profiler software (the BeamLux II, Metrolux). The higher luminous intensity is presented with a white-colored region, and less with a red-

colored one. It indicates that the radiative recombinations in LED B occur mostly around the edge of p- and n-pads (red

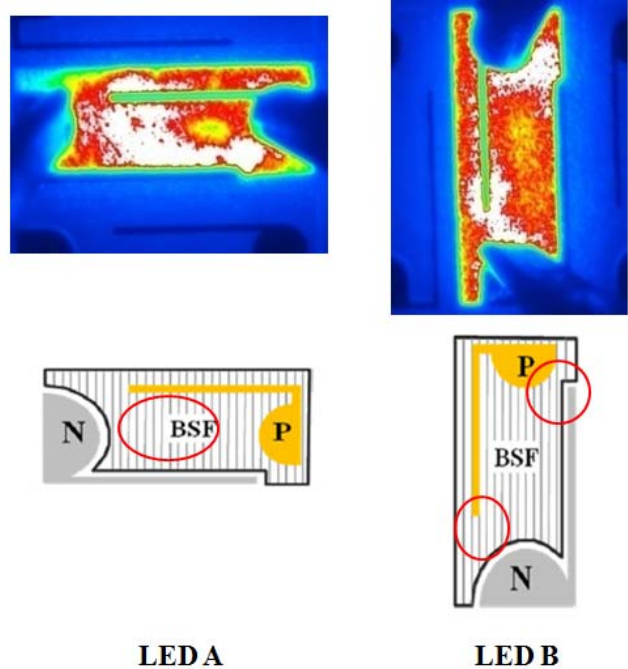


Figure 6. Images of spatial light distributions of LEDs parallel to c- and m-axes

circles), possibly due to nonuniform current spreading in cladding layer. In the case of LED A, lights are more uniformly emitted in the area between p- and n-pads (red circle). Thus, it is found that BPSFs significantly affect the carrier transport in faulted a-plane GaN films, resulting in the nonuniform current spreading of heteroepitaxial nonpolar GaN LEDs. Optimization of chip design considering the carrier scattering by BPSFs will lead to better performance of nonpolar GaN LEDs.

CONCLUSIONS

Effects of BPSFs on the electrical and optical anisotropies of nonpolar a-plane GaN LEDs on r-plane sapphire substrates were investigated. The lowest specific contact resistances of $\sim 10^{-5} \Omega \cdot \text{cm}^2$ were obtained when annealed at $\sim 700^\circ\text{C}$ under nitrogen environment. The sheet resistance along the c-axis was measured to be two times higher than the one along the m-axis, possibly due to the carrier scatterings by BPSFs in the direction perpendicular to the c-axis. It is also shown that the output powers of nonpolar a-plane GaN LEDs are significantly influenced by the presence of BPSFs, which laterally hamper the carrier transport in the n-GaN layer, especially in the direction parallel to the c-axis in faulted nonpolar nitride films.

ACKNOWLEDGEMENTS

This research was supported by Basic Science Research Program through the National Research Foundation of Korea(NRF) funded by the Ministry of Education, Science and Technology (2010-0004968).

REFERENCES

- [1] R. T. Tung, Phys. Rev. B **45**, 13509 (1992).
- [2] R. Ther, et al., *Sample Paper Reference with Title*, 1999 GaAs MANTECH Technical Digest, pp. 103-107, April 1999.
- [1] J. S. Speck and S F Chhibu, Non-Polar and Semipolar Group III Nitride-Based Materials MRS Bull. **34**, 304 (2009).
- [2] C. Chen, V. Adivararahan, J. Yang, M. Shatalov, E. Kuokstis and M. Asif Khan, Jpn. J. Appl. Phys. **42**, L1039(2003).
- [3] Y. Wang, F. Ren, W. Lim, S. J. Pearton, K. H. Baik, S. Hwang, Y. G. Seo, and S. Jang, Curr Appl Phys. **10**, 1029 (2010).
- [4] D. N. Zakharov, Z. Liliental-Weber, B. Wagner, Z. J. Reitmeier, E. A. Preble, and R. F. Davis, Phys. Rev. B. **71**, 235334 (2005).
- [5] P. P. Paskov, T. Paskova, B. Monemar, S. Figge, D. Hommel, B. A. Haskell, P. T. Fini, J. S. Speck, and S. Nakamura, Superlattices Microstructures. **40**, 253 (2006).
- [6] C. Stampfl and C. G. Van de Walle, Phys. Rev. B. **57**, R15052 (1998).
- [7] Y. T. Rebane, Y. G. Shreter, and M. Albrecht, Phys. Status Solidi A. **164**, 141 (1997).
- [8] K. H. Baik, Y. G. Seo, S. Hong, S. Lee, J. Kim, J. Son, and S. Hwang, IEEE Photon. Technol. Lett. **22**, 1041 (2010).
- [9] K. H. Baik, Y. G. Seo, J. Kim, S. Hwang, W. Lim, C. Y. Chang, S. J. Pearton, F. Ren, and S. Jang, J. Phys. D: Appl. Phys. **43**, 295102 (2010).
- [10] S. Hwang, Y. G. Seo, K. H. Baik, I. Cho, J. H. Baek, S. Jung, T. G. Kim, and M. Cho, Appl. Phys. Lett., **95**, 071101(2009).
- [11] M. McLaurin, T. E. Mates, F. Wu, and J. S. Speck, J. Appl. Phys., **100**, 063707 (2006).
- [12] M. McLaurin and J.S. Speck. Phys. Stat. Sol. (RRL) **1**. No. 3, 110 (2007).

ACRONYMS

TLM: transfer line method
BPSF: basal plane stacking fault
QCSE: quantum-confined Stark effect
QW: quantum well
LED: light-emitting diode
PSF: prismatic stacking fault